

Supplemental Figures for:

Endothelial alpha globin is a nitrite reductase

T.C. Stevenson Keller IV^{1,2}
Christophe Lechaue³
Alexander S. Keller^{1,4}
Gilson Brás Broseghini-Filho^{1,5}
Joshua T. Butcher⁶
Henry R. Askew Page¹
Aditi Islam¹
Zhe Yin Tan¹
Leon J. DeLalio^{1,4}
Steven Brooks⁷
Poonam Sharma⁸
Kwangseok Hong⁹
Wenhao Xu¹⁰
Alessandra Simão Padilha⁵
Claire A. Ruddiman^{1,4}
Angela K. Best¹
Edgar Macal¹
Daniel B. Kim-Shapiro¹¹
George Christ⁸
Zhen Yan¹
Miriam M. Cortese-Krott¹²
Karina Ricart¹³
Rakesh Patel¹³
Timothy P. Bender¹⁴
Swapnil K. Sonkusare^{1,2}
Mitchell J. Weiss³
Hans Ackerman⁷
Linda Columbus^{2,15}
Brant E. Isakson^{1,2 *}

¹ Robert M Berne Cardiovascular Research Center, University of Virginia School of Medicine, Charlottesville, VA

² Department of Molecular Physiology and Biophysics, University of Virginia School of Medicine, Charlottesville, VA

³ Department of Hematology, St. Jude Children's Research Hospital, Memphis, TN

⁴ Department of Pharmacology, University of Virginia School of Medicine, Charlottesville, VA

⁵ Department of Physiological Sciences, Federal University of Espirito Santo, Brazil

⁶ Department of Physiological Sciences, College of Veterinary Medicine, Oklahoma State University, Stillwater, OK

⁷ Physiology Unit, Laboratory of Malaria and Vector Research, National Institute of Allergy and Infectious Diseases, Bethesda, MD

⁸ Department of Biomedical Engineering, University of Virginia, Charlottesville, VA

⁹ Department of Physical Education, College of Education, Chung-Ang University, Seoul South Korea

¹⁰ Transgenic Mouse Facility, Department of Medicine, University of Virginia School of Medicine, Charlottesville, VA

¹¹ Department of Physics, Translational Science Center, Wake Forest University, Winston-Salem, NC

¹² Cardiovascular Research Laboratory, Division of Cardiology, Pneumology and Angiology, Medical Faculty, Heinrich Heine University, Düsseldorf, Germany

¹³ Department of Pathology, University of Alabama at Birmingham, Birmingham, AL

¹⁴ Department of Microbiology, Immunology and Cancer, University of Virginia School of Medicine, Charlottesville, VA

¹⁵ Department of Chemistry, University of Virginia, Charlottesville, VA

** To whom correspondence should be addressed*

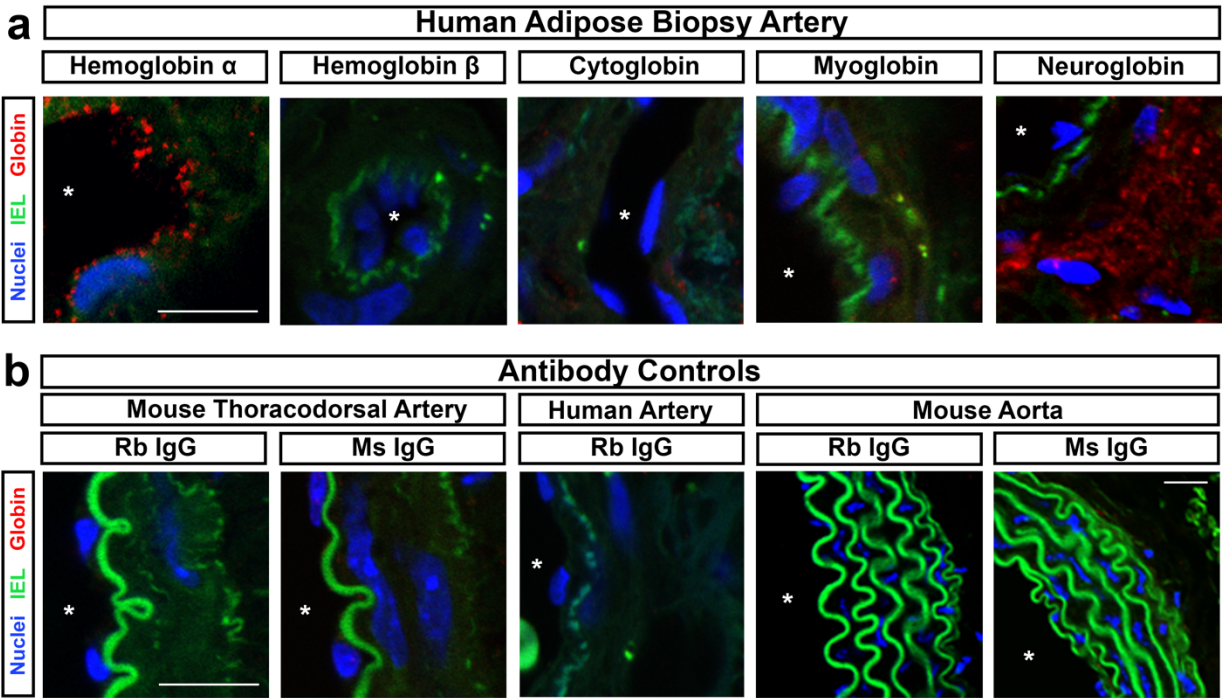
University of Virginia School of Medicine

Charlottesville, VA 22908 USA

E: brant@virginia.edu

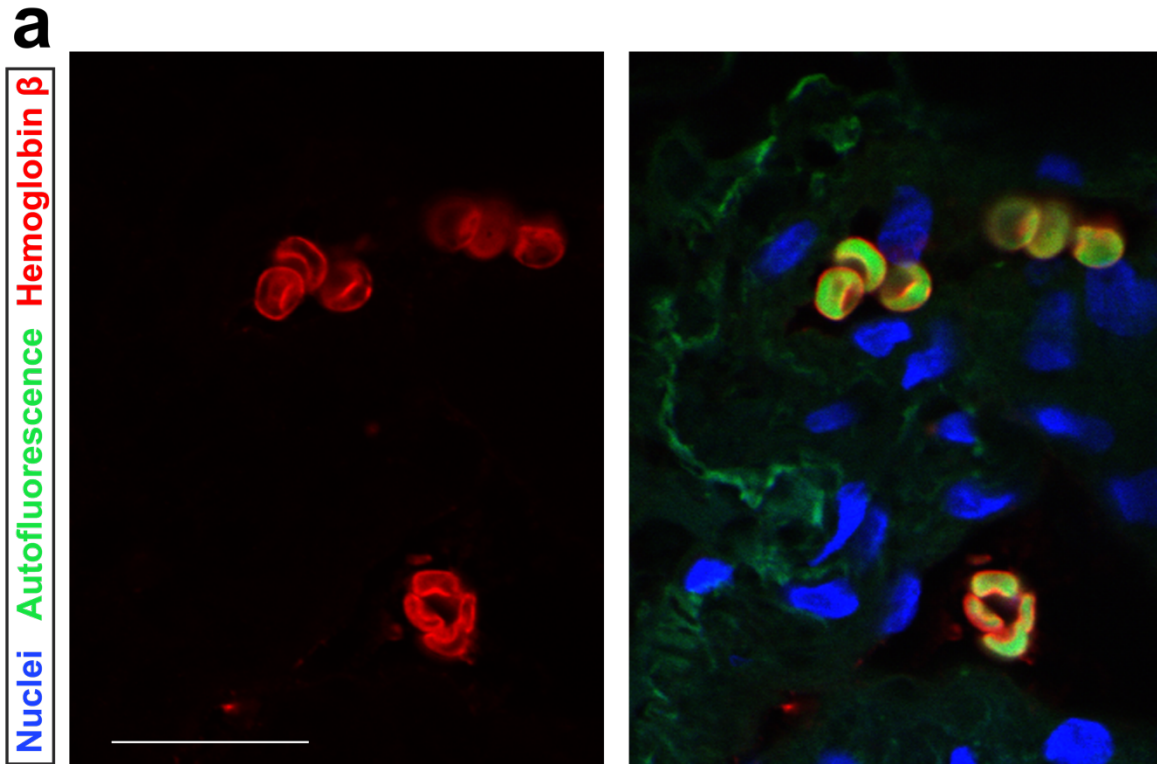
P: 434-924-2093

Supplemental Figure 1:



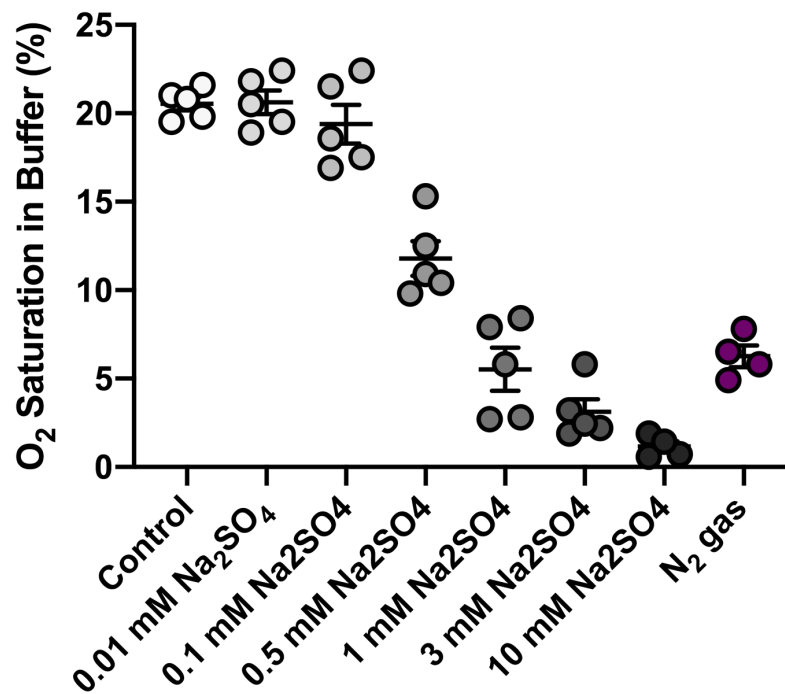
*SUPPLEMENTAL FIGURE 1: Alpha globin is expressed in the endothelium of arterioles from human adipose biopsy samples. (a) Expression of alpha globin in the endothelium is observed from human adipose biopsy samples. No other globin was detected in the endothelium; neuroglobin signal was observed in the adventitial layers. (b) Antibody controls for the positive signals seen in the tissues in Main Text Figure 1 and in this figure, demonstrating the specificity of the staining. In all images, an asterisk indicates the lumen of the vessel. The scale bars in panel **a** represent 10 μm , those in panel **b** represent 25 μm . The images are representative of the analysis of at least four individuals in each case.*

Supplemental Figure 2:



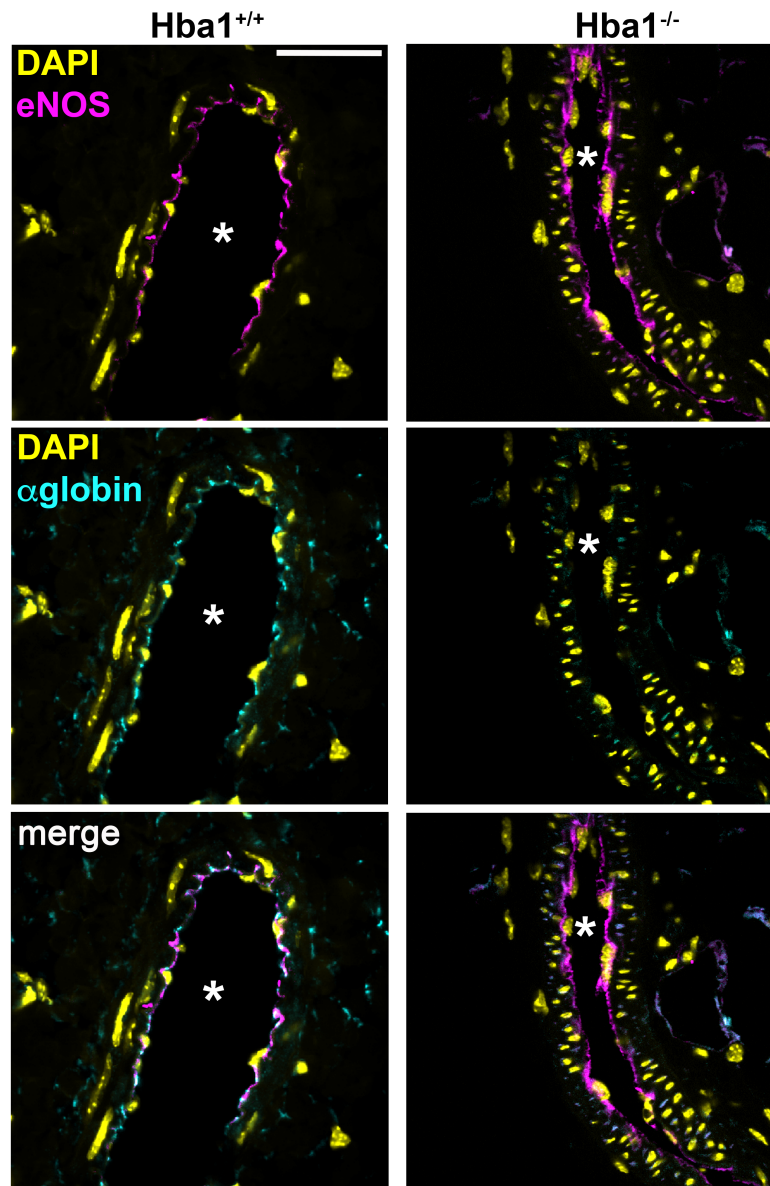
SUPPLEMENTAL FIGURE 2: Staining for hemoglobin β in erythrocytes, as an immunohistochemistry positive control. (a) Positive signal (red) for hemoglobin β is observed in erythrocytes captured in a section of a human adipose biopsy. Erythrocytes are strongly autofluorescent (green), and nuclei are stained with DAPI (blue). These results are representative of at least 3 independent experiments. The scale bar represents 30 μm .

Supplemental Figure 3:



SUPPLEMENTAL FIGURE 3: Oxygen content of buffer treatments with sodium dithionite as used in the experiments. Increasing doses of Na₂S₂O₄ decrease the O₂ saturation in the KREBS-based buffer used for the vasoreactivity experiments. The single dose of 1 mM Na₂S₂O₄ used in our studies produces an aqueous O₂ saturation similar to that obtained by bubbling the solution with pure nitrogen gas. For each condition, the O₂ saturation was measured in n = 5 samples. Bar graphs are centered on mean with error bars denoting standard error. Source data are provided in the source data file.

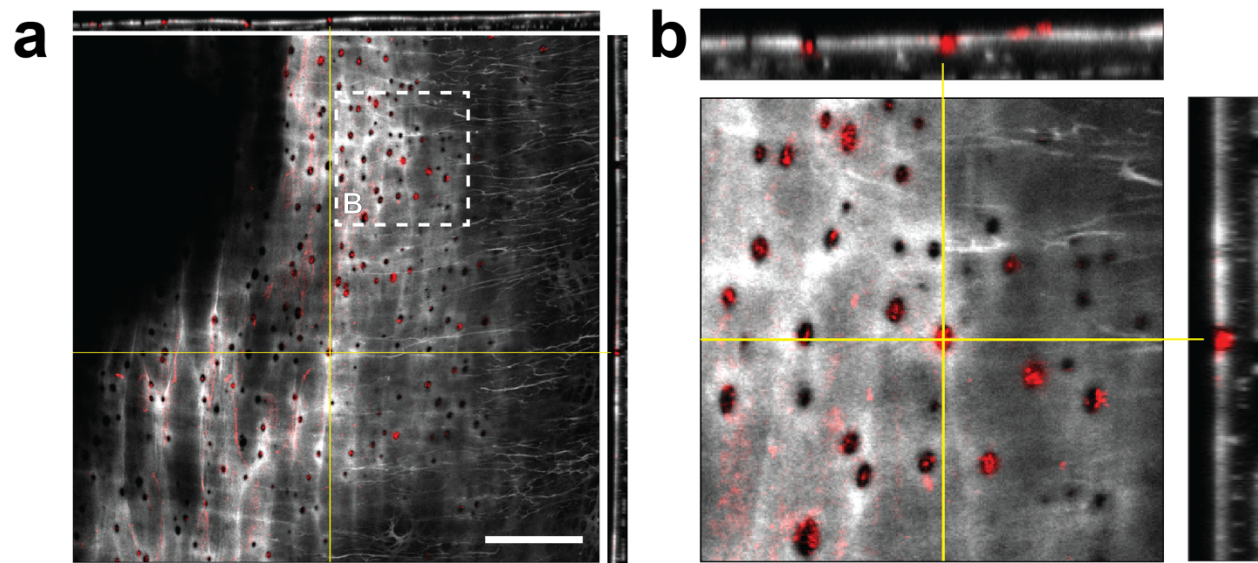
Supplemental Figure 4:



SUPPLEMENTAL FIGURE 4: Loss of endothelial alpha globin in the Hba1^{-/-} model.

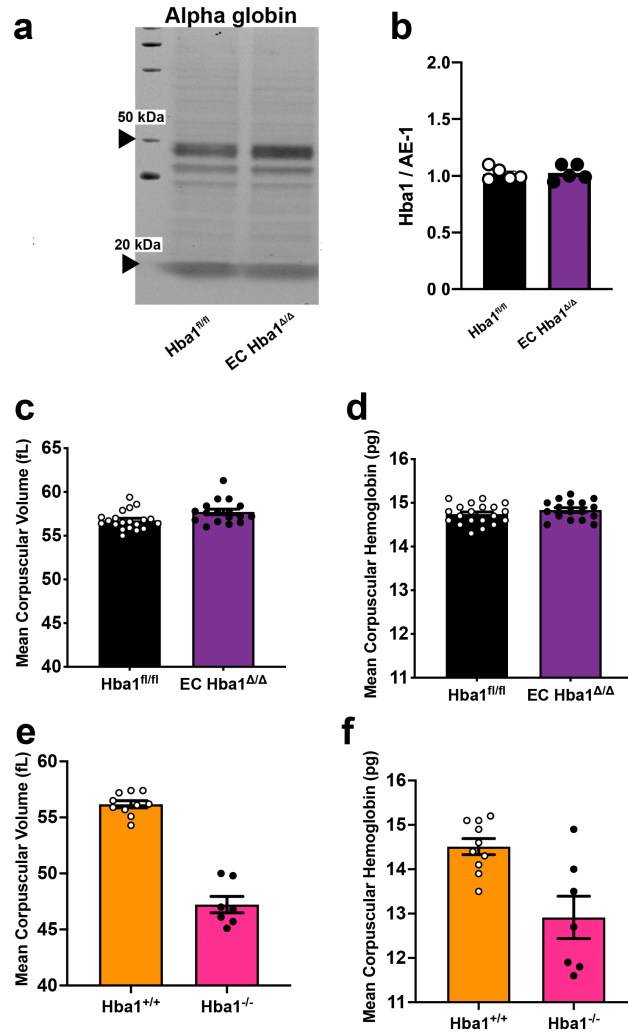
Immunohistochemical staining for eNOS (top, magenta) and alpha globin (middle, cyan) in the *Hba1^{+/+}* (left) and *Hba1^{-/-}* (right) animals. The bottom row shows all channels (including that for DAPI [yellow]) merged. Alpha globin signal is absent from the endothelium of *Hba1^{-/-}* vessels. In each image, an asterisks indicates the lumen of the vessel. The scale bar in the top left image represents 50μm. Images are representative of n = 5 samples analyzed for each genotype.

Supplemental Figure 5:



SUPPLEMENTAL FIGURE 5: *Localization of alpha globin to the holes in the internal elastic lamina.* Confocal microscopic analysis of the expression of alpha globin in *en face* preparations shows that alpha globin is localized to the holes in the internal elastic lamina at a site called the myoendothelial junction. **(a)** Low-power image showing many holes in the internal elastic lamina (gray) with alpha globin (red fluorescent signal) expression inside. **(b)** High-power image of the boxed region in panel **a**. Yellow lines indicate the planes of analysis in the XZ and YZ projections shown, respectively, on the top and right of the main image. Scale bar in **a** represents 50 μm . These images are representative of 6 independent experiments.

Supplemental Figure 6:



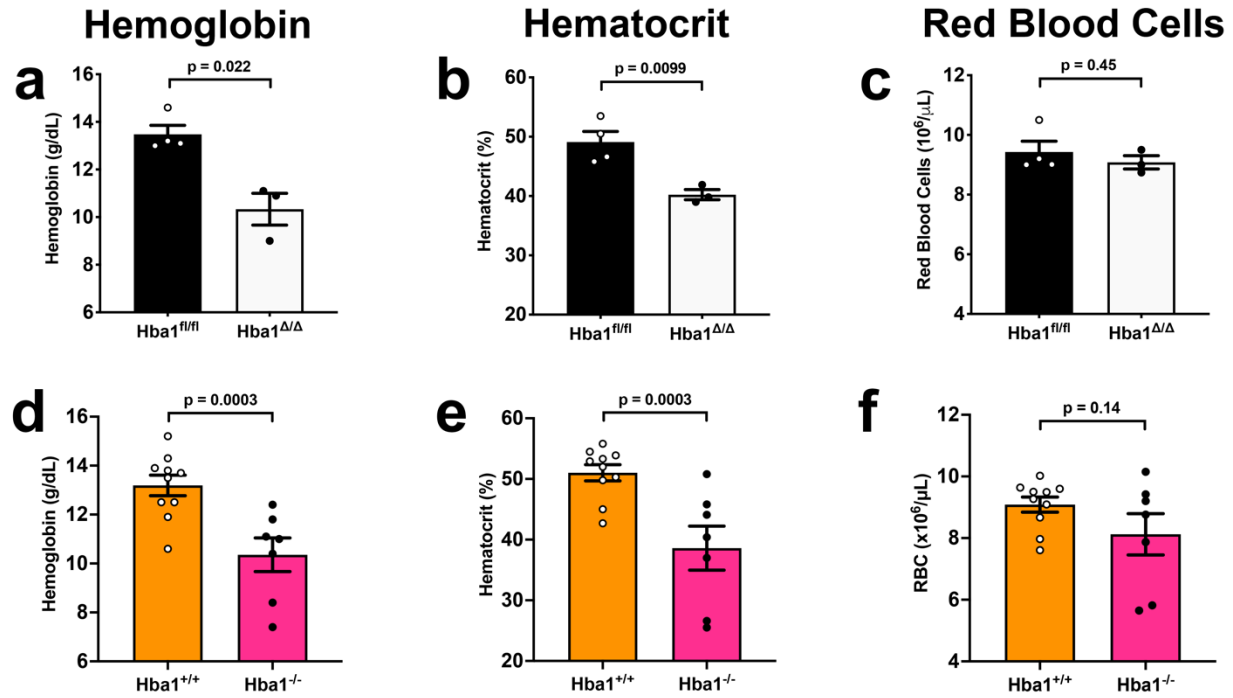
SUPPLEMENTAL FIGURE 6: Additional hematologic measurements for the EC *Hba1*^{Δ/Δ} model.

(a) Expression of alpha globin within the erythrocytes was unchanged in the EC *Hba1*^{Δ/Δ} mice. This uncropped Western blot of alpha globin protein (~18 kDa) shows similar expression levels in the *Hba1*^{fl/fl} and EC *Hba1*^{Δ/Δ} mice. (b) Normalization of alpha globin protein to AE1 protein levels is shown (n = 5 for each quantification). (c, d) Mean corpuscular volume (MCV) (c) or mean corpuscular hemoglobin (MCH) (d) were not changed as a result of endothelial-specific (*Cdh5-Cre*^{ERT2}) recombination of the *Hba1*^{fl/fl} allele. (e, f) In the neomycin-insertion global deletion (*Hba1*^{-/-}) mice, both MCV (e) and MCH (f) are decreased compared to WT controls. For these experiments, n = 20 *Hba1*^{fl/fl} mice, n = 17 EC *Hba1*^{Δ/Δ} mice, n = 10 *Hba1*^{+/+} mice, and n = 7 *Hba1*^{-/-}

4 mice were used. Bar graphs are centered on mean with error bars denoting standard error.

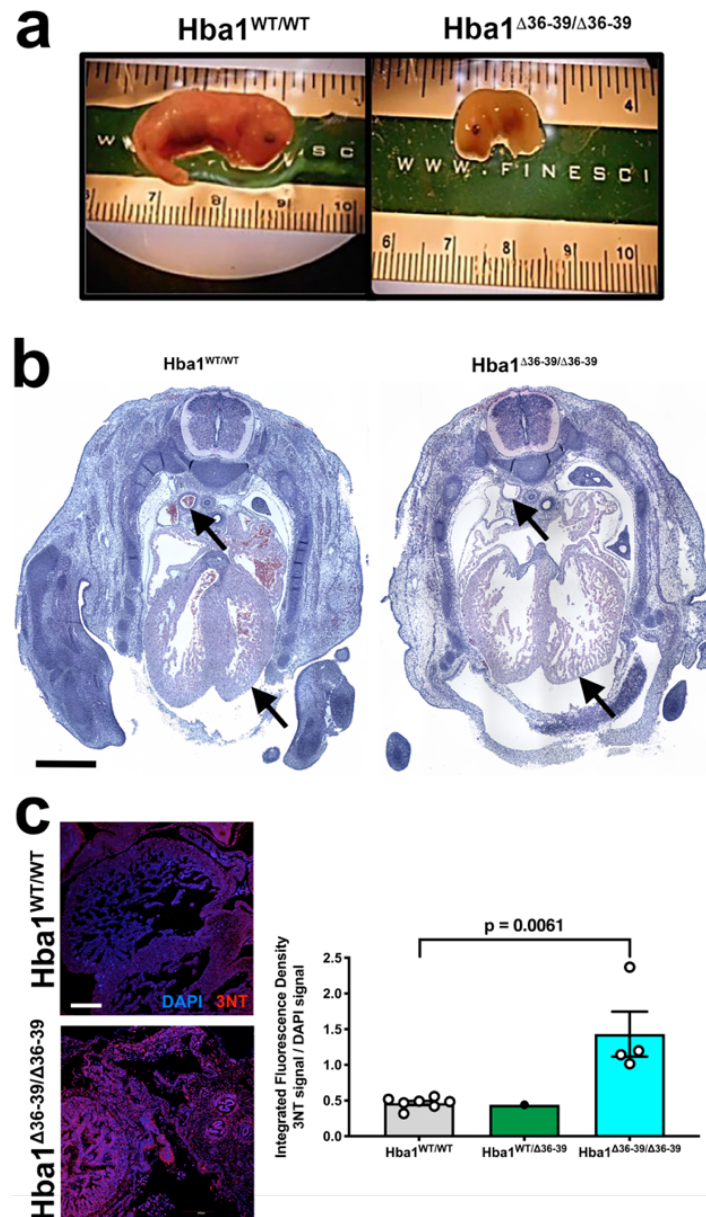
Source data are provided in the source data file.

Supplemental Figure 7:



SUPPLEMENTAL FIGURE 7: Blood parameters of mice with global deletion of *Hba1* show anemic phenotype. Hemoglobin (a, d), hematocrit (b, e), and total RBC (c, f) show the same patterns in a global *Hba1* KO ($Hba1^{fl/fl}; Sox2-Cre$, denoted as $Hba1^{\Delta/\Delta}$) and a model of alpha thalassemia ($Hba1^{-/-}$). For these experiments, $n = 4$ $Hba1^{fl/fl}$ mice, $n = 3$ $Hba1^{\Delta/\Delta}$ mice, $n = 10$ $Hba1^{+/+}$ mice, and $n = 7$ for $Hba1^{-/-}$ mice were used. Results were compared with one-sided t-tests. Bar graphs are centered on mean with error bars denoting standard error. Source data are provided in the source data file.

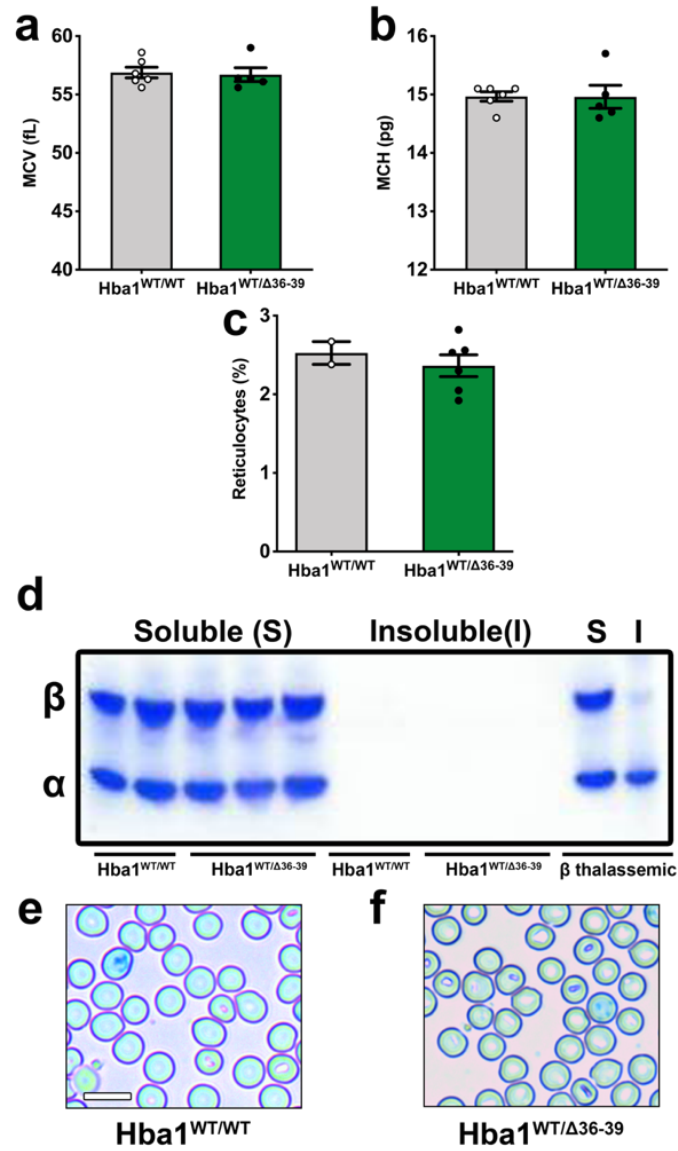
Supplemental Figure 8:



SUPPLEMENTAL FIGURE 8: *Homozygous Hba1^{Δ36-39} mutation is embryonically lethal, with pathologic nitrotyrosine formation.* (a) Embryos with the homozygous Hba1^{Δ36-39} mutation are already deceased at approximately E14.5, showing stunted growth. (b) Gross histology shows cardiac non-compaction, lack of blood, and dilated major vessels (arrows). The scale bar represents 5 mm. This image is representative of 4 independent animals. (c) Immunostaining for 3-nitrotyrosine (a pathologic marker of excess reactive nitrogen species), shows a large increase

in signal in embryos with homozygous $Hba1^{\Delta36-39}$ mutation, as compared to WT or heterozygous embryos. Heart and trunk vasculature is shown. The scale bar represents 20 μm . For the nitrotyrosine quantification in panel **c**, $n = 7$ $Hba1^{WT/WT}$ mice, $n = 1$ $Hba1^{WT/\Delta36-39}$ mice, and $n = 4$ $Hba1^{\Delta36-39/\Delta36-39}$ mice were used. Results for $Hba1^{WT/WT}$ and $Hba1^{\Delta36-39/\Delta36-39}$ mice were compared with a one-sided t-test. Bar graphs are centered on mean with error bars denoting standard error. Source data are provided in the source data file.

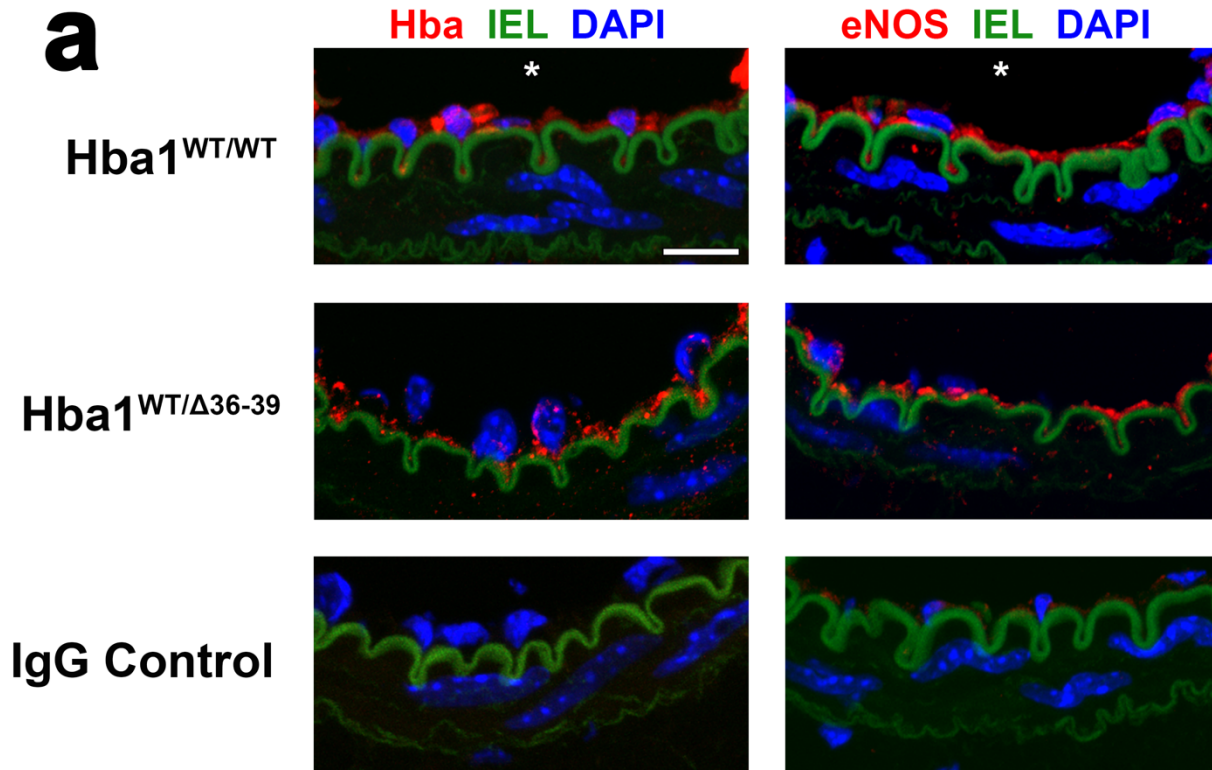
Supplemental Figure 9:



SUPPLEMENTAL FIGURE 9: $Hba1^{WT/\Delta36-39}$ adults display unchanged red cell and reticulocyte characteristics, with no observed insoluble hemoglobin. (a–c) Blood cell parameters, including mean corpuscular volume (a), mean corpuscular hemoglobin (b), and number of reticulocytes (c), did not differ between WT and heterozygous $Hba1^{\Delta36-39}$ mutants. (d) Blood samples from WT and $Hba1^{\Delta36-39}$ mutants showed no insoluble hemoglobin. The band corresponding to beta globin is at the top of the gel; the lower band is alpha globin. Insoluble alpha globin was observed in control

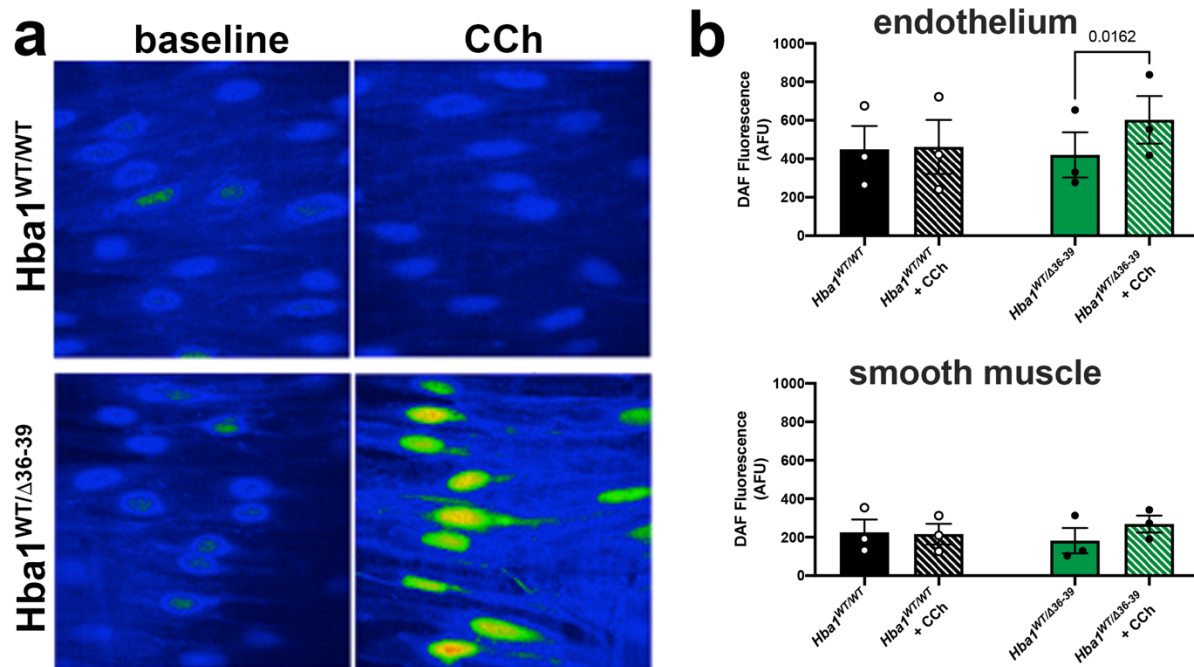
sample from a model of beta thalassemia (far right). This experiment is representative of 3 independent experiments on the same samples. (e, f) Cresyl blue staining of a blood smear, demonstrating that heterozygous $Hba1^{WT/\Delta36-39}$ mutants showed no appreciable increase in reticulocytes or precipitated hemoglobin as compared to $Hba1^{WT/WT}$ controls. The scale bar represents 5 μ m. For the experiments in panels a and b, n = 6 $Hba1^{WT/WT}$ mice, n = 5 $Hba1^{WT/\Delta36-39}$ mice were used. For the experiments in panel c, n = 2 $Hba1^{WT/WT}$ mice and n = 6 $Hba1^{WT/\Delta36-39}$ mice were used. Means were compared with a t-test. Bar graphs are centered on mean with error bars denoting standard error. Source data are provided in the source data file.

Supplemental Figure 10:



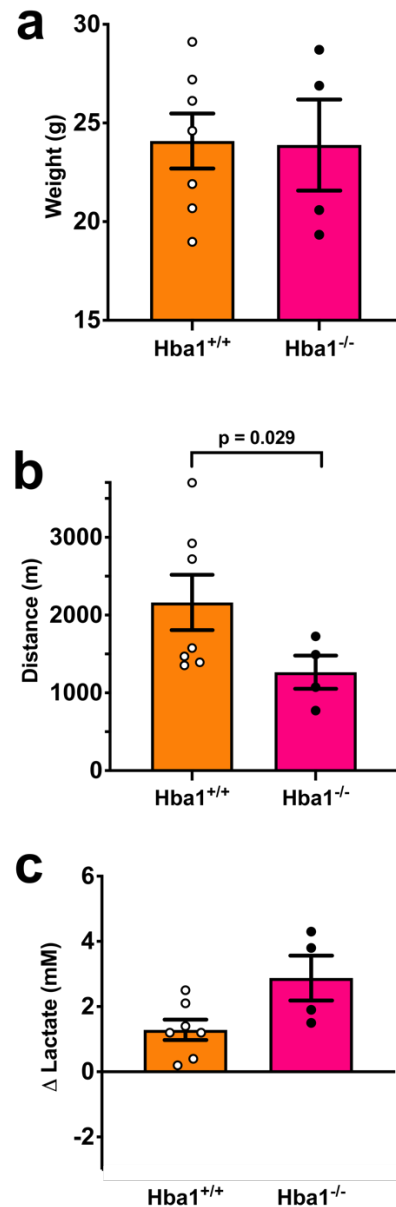
SUPPLEMENTAL FIGURE 10: a, Alpha globin and eNOS are expressed at similar levels in Hba1^{WT/WT} and Hba1^{WT/Δ36-39} adult tissues. (a) Immunostaining controls for PLA. Alpha globin (left) and eNOS (right) are expressed and detectable at similar levels in the thoracodorsal arteries of Hba1^{WT/WT} and Hba1^{WT/Δ36-39} mice. The scale bar represents 20 μm. The sections in the bottom row are stained with non-reactive IgG from the primary antibody host animal and shows no signal for either antigen. These images are representative of four individual animals from this experiment.

Supplemental Figure 11:



SUPPLEMENTAL FIGURE 11: Increased nitric oxide generation in mice lacking an eNOS binding site in their alpha globin. (a) *En face* imaging of third-order mesenteric arterioles that were loaded with DAF and were subjected to 10 μ M carbachol (CCh) stimulation and (b) the data quantified in the optical slices of endothelium or smooth muscle. Cross-hatched bar graphs represent the CCh-stimulated condition. All measurements were performed with $n = 3$ mice, with several fields of view in each artery averaged for one replicate value. Littermate groups were compared with a paired t-test. P-values less than 0.05 are shown. Bar graphs are centered on mean with error bars denoting standard error. Source data are provided in the source data file.

Supplemental Figure 12:

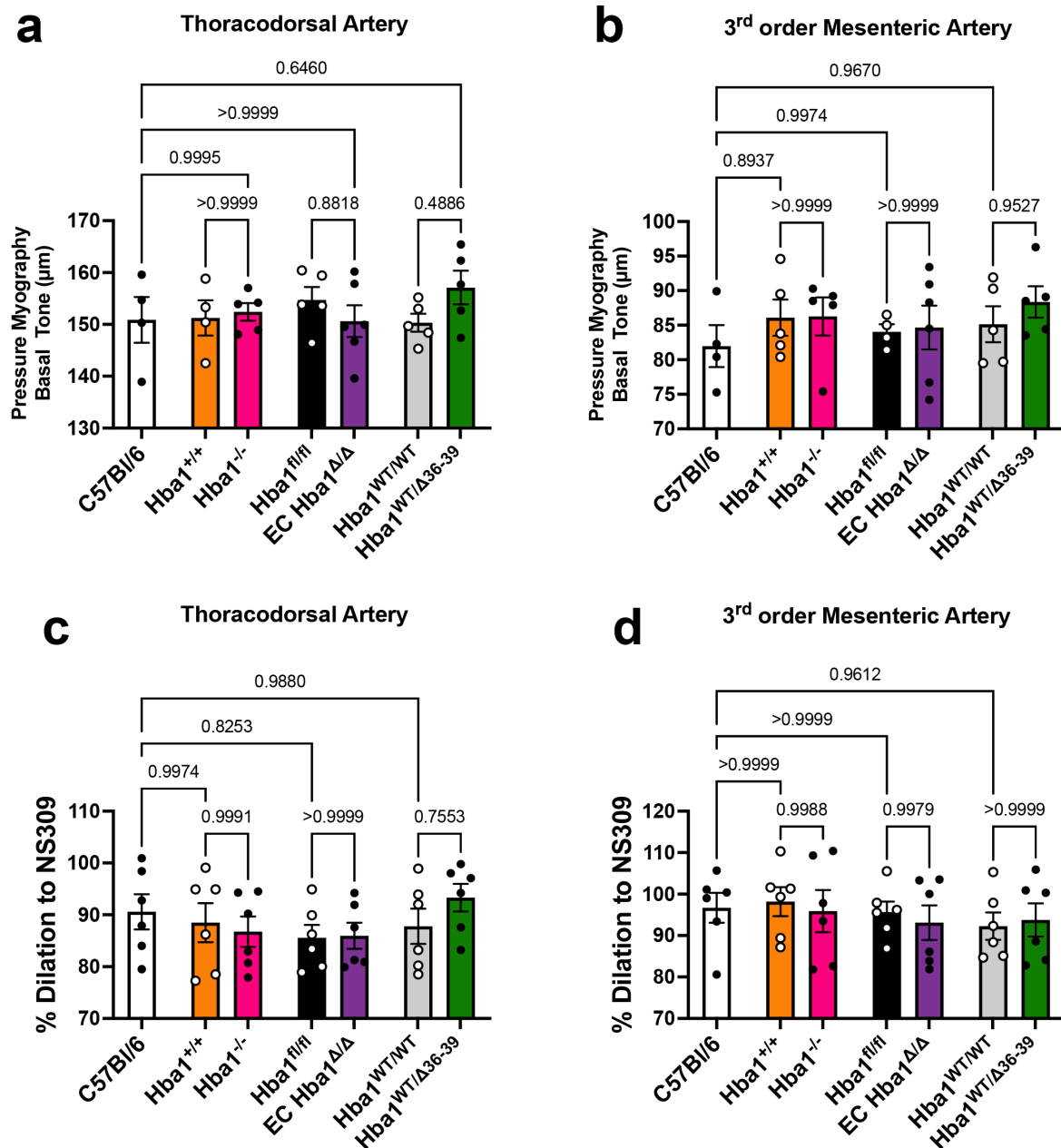


SUPPLEMENTAL FIGURE 12: Global deletion of *Hba1* reduces exercise capacity. Mice with a constitutive, global knockout of *Hba1* had similar weight to *Hba1*^{+/+} controls (a) but decreased exercise capacity (b), with increased blood lactate (c). The significant defect in running distance could be related to the anemia observed in these mice (Supplementary Figure 7). For these experiments, *n* = 7 *Hba1*^{+/+} mice and *n* = 4 for *Hba1*^{-/-} mice were used. Results were compared

with a one-sided t-test. Bar graphs are centered on mean with error bars denoting standard error.

Source data are provided in the source data file.

Supplemental Figure 13:



SUPPLEMENTAL FIGURE 13: Basal tone of the vessels was not different for littermate control groups. Basal lumen diameter of the thoracodorsal artery (a) and third-order mesenteric artery (b) from the experimental genotypes and their littermate controls. (c, d) The dilation of thoracodorsal arteries (c) and third-order mesenteric arteries (d) from the indicated genotypes were subjected to a single dose of 1 μM NS309 to evaluate maximum dilation. The P-values for

comparisons are shown. The groups were compared with a one-way ANOVA. Bar graphs are centered on mean with error bars denoting standard error. Source data are provided in the source data file.

Supplemental Table 1: Genotypes of P21 pups from five breeding pairs of *Hba1^{fl/+}* mice. P-values were determined with a χ^2 test.

<i>Hba1^{fl/+} × Hba1^{fl/+}</i>				
Mating Pair	Litter	<i>Hba1^{fl/fl}</i>	<i>Hba1^{fl/+}</i>	<i>Hba1^{WT}</i>
1	1	1	4	2
	2	2	4	2
2	1	3	2	3
	2	3	3	2
3	1	2	4	2
	2	2	3	2
4	1	1	4	1
	2	3	1	3
5	1	1	4	2
	2	2	5	1
Total		20	34	20
Percentage		27	46	27
<i>P</i>-value range: 0.10 - 0.90				

Supplemental Table 2: Genotypes of P21 pups from four breeding pairs of *Hba1^{fl/+}; Cdh5-Cre^{ERT2}* mice. P-values were determined with a χ^2 test.

<i>Hba1^{fl/+}; Cdh5-Cre^{ERT2} × Hba1^{fl/+}; Cdh5-Cre^{ERT2}</i>				
Mating Pair	Litter	<i>Hba1^{fl/fl}; Cdh5-Cre^{ERT2}</i>	<i>Hba1^{fl/+}; Cdh5-Cre^{ERT2}</i>	<i>Hba1^{+/+}; Cdh5-Cre^{ERT2}</i>
1	1	1	5	2
	2	3	2	2
2	1	2	2	3
	2	3	3	1
	3	3	4	0
3	1	1	4	1
	2	1	4	3
	3	4	2	3
4	1	0	5	2
	2	1	3	2
Total		19	34	19
Percentage		26.4	47.2	26.4
<i>P</i>-value range: 0.975 - 0.99				

Supplemental Table 3: Genotypes of P21 pups from three breeding pairs of *Hba1^{fl/+}*; *Sox2-Cre* mice. P-values were determined with a χ^2 test.

<i>Hba1^{fl/+}</i>; <i>Sox2-Cre</i> × <i>Hba1^{fl/+}</i>; <i>Sox2-Cre</i>				
Mating Pair	Litter	<i>Hba1^{fl/fl}</i>; <i>Sox2-Cre</i>	<i>Hba1^{fl/+}</i>; <i>Sox2-Cre</i>	<i>Hba1^{+/+}</i>; <i>Sox2-Cre</i>
1	1	1	5	0
	2	1	3	1
	3	1	3	1
	4	1	3	1
	5	0	3	3
2	1	0	3	3
	2	1	3	2
3	1	1	3	2
	2	1	3	2
	3	1	3	3
Total		8	32	18
Percentage		13.7	55.2	31.1
<i>P</i>-value range: 0.1 - 0.9				

Supplemental Table 4: Genotypes of P21 pups from three breeding pairs of *Hba1^{+/-neo}* mice. P-values were determined with a χ^2 test.

<i>Hba1^{+/-neo}</i> × <i>Hba1^{+/-neo}</i>				
Mating Pair	Litter	<i>Hba1^{neo/neo}</i>	<i>Hba1^{+/-neo}</i>	<i>Hba1^{+/+}</i>
1	1	0	4	2
	2	1	3	1
	3	1	3	2
	4	1	6	0
2	1	1	4	2
	2	0	5	3
	3	1	3	1
3	1	0	3	3
	2	1	2	2
	3	1	2	3
Total		7	35	19
Percentage		11.5	57.4	31.1

<i>P</i> -value range: 0.025 - 0.05			
-------------------------------------	--	--	--

Supplemental Table 5: Genotypes of P21 pups from three breeding pairs of *Hba1*^{WT/Δ36-39} mice. P-values were determined with a χ^2 test.

<i>Hba1</i> ^{WT/Δ36-39} × <i>Hba1</i> ^{WT/Δ36-39}				
Mating Pair	Litter	<i>Hba1</i> ^{Δ36-39/Δ36-39}	<i>Hba1</i> ^{WT/Δ36-39}	<i>Hba1</i> ^{WT/WT}
1	1	0	4	4
	2	0	2	3
	3	0	2	3
	4	0	2	5
	5	0	3	3
2	1	0	4	4
	2	0	2	2
	3	0	2	3
	4	0	3	3
3	1	1	4	1
Total		1	28	31
Percentage		1.67	46.67	51.67
<i>P</i> -value < 0.005				